Belle-preprint 2005-2
KEK Preprint 2004-93
Intended for *PLB*
Author: K.Hayasaka, T. Ohshima

Search for $\tau \to e\gamma$ decay at Belle

K. Hayasaka,[19] K. Abe,[6] K. Abe,[38] H. Aihara,[40] Y. Asano,[44] T. Aushev,[10] S. Bahinipati,[4] A. M. Bakich,[35] I. Bedny,[1] U. Bitenc,[11] I. Bizjak,[11] S. Blyth,[23] A. Bondar,[1] A. Bozek,[24] M. Bračko,[6,17,11] J. Brodzicka,[24] T. E. Browder,[5] M.-C. Chang,[23] P. Chang,[23] A. Chen,[21] W. T. Chen,[21] B. G. Cheon,[3] R. Chistov,[10] Y. Choi,[34] Y. K. Choi,[34] A. Chuvikov,[31] J. Dalseno,[18] M. Dash,[45] S. Eidelman,[1] Y. Enari,[19] D. Epifanov,[1] S. Fratina,[11] N. Gabyshev,[1] A. Garmash,[31] T. Gershon,[6] G. Gokhroo,[36] J. Haba,[6] H. Hayashii,[20] M. Hazumi,[6] L. Hinz,[15] T. Hokuue,[19] Y. Hoshi,[38] S. Hou,[21] W.-S. Hou,[23] T. Iijima,[19] A. Imoto,[20] K. Inami,[19] A. Ishikawa,[6] M. Iwasaki,[40] Y. Iwasaki,[6] J. H. Kang,[46] J. S. Kang,[13] S. U. Kataoka,[20] N. Katayama,[6] H. Kawai,[2] T. Kawasaki,[26] H. R. Khan,[41] H. Kichimi,[6] H. J. Kim,[14] J. H. Kim,[34] S. K. Kim,[33] S. M. Kim,[34] P. Krokovny,[1] C. C. Kuo,[21] A. Kuzmin,[1] Y.-J. Kwon,[46] G. Leder,[9] S. E. Lee,[33] S. H. Lee,[33] T. Lesiak,[24] J. Li,[32] S.-W. Lin,[23] F. Mandl,[9] T. Matsumoto,[42] A. Matyja,[24] W. Mitaroff,[9] K. Miyabayashi,[20] H. Miyake,[28] H. Miyata,[26] T. Nagamine,[39] Y. Nagasaka,[7] E. Nakano,[27] M. Nakao,[6] Z. Natkaniec,[24] S. Nishida,[6] O. Nitoh,[43] S. Ogawa,[37] T. Ohshima,[19] T. Okabe,[19] S. Okuno,[12] S. L. Olsen,[5] W. Ostrowicz,[24] P. Pakhlov,[10] H. Palka,[24] C. W. Park,[34] N. Parslow,[35] R. Pestotnik,[11] L. E. Piilonen,[45] N. Root,[1] H. Sagawa,[6] Y. Sakai,[6] N. Sato,[19] T. Schietinger,[15] O. Schneider,[15] J. Schümann,[23] K. Senyo,[19] H. Shibuya,[37] B. Shwartz,[1] V. Sidorov,[1] A. Somov,[4] N. Soni,[29] R. Stamen,[6] S. Stanič,[47,*] M. Starič,[11] K. Sumisawa,[28] T. Sumiyoshi,[42] S. Y. Suzuki,[6] O. Tajima,[6] F. Takasaki,[6] N. Tamura,[26] M. Tanaka,[6] Y. Teramoto,[27] X. C. Tian,[30] T. Tsuboyama,[6] T. Tsukamoto,[6] S. Uehara,[6] T. Uglov,[10] S. Uno,[6] G. Varner,[5] S. Villa,[15] C. C. Wang,[23] C. H. Wang,[22] M. Watanabe,[26] A. Yamaguchi,[39] Y. Yamashita,[25] M. Yamauchi,[6] Heyoung Yang,[33] Y. Yuan,[8] L. M. Zhang,[32] Z. P. Zhang,[32] V. Zhilich,[1] and D. Žontar[16,11]

(Belle Collaboration)

[1]*Budker Institute of Nuclear Physics, Novosibirsk, Russia*
[2]*Chiba University, Chiba, Japan*
[3]*Chonnam National University, Kwangju, South Korea*
[4]*University of Cincinnati, Cincinnati, OH, USA*
[5]*University of Hawaii, Honolulu, HI, USA*
[6]*High Energy Accelerator Research Organization (KEK), Tsukuba, Japan*
[7]*Hiroshima Institute of Technology, Hiroshima, Japan*
[8]*Institute of High Energy Physics, Chinese Academy of Sciences, Beijing, PR China*
[9]*Institute of High Energy Physics, Vienna, Austria*
[10]*Institute for Theoretical and Experimental Physics, Moscow, Russia*
[11]*J. Stefan Institute, Ljubljana, Slovenia*
[12]*Kanagawa University, Yokohama, Japan*
[13]*Korea University, Seoul, South Korea*
[14]*Kyungpook National University, Taegu, South Korea*
[15]*Swiss Federal Institute of Technology of Lausanne, EPFL, Lausanne, Switzerland*
[16]*University of Ljubljana, Ljubljana, Slovenia*

[17]University of Maribor, Maribor, Slovenia
[18]University of Melbourne, Victoria, Australia
[19]Nagoya University, Nagoya, Japan
[20]Nara Women's University, Nara, Japan
[21]National Central University, Chung-li, Taiwan
[22]National United University, Miao Li, Taiwan
[23]Department of Physics, National Taiwan University, Taipei, Taiwan
[24]H. Niewodniczanski Institute of Nuclear Physics, Krakow, Poland
[25]Nihon Dental College, Niigata, Japan
[26]Niigata University, Niigata, Japan
[27]Osaka City University, Osaka, Japan
[28]Osaka University, Osaka, Japan
[29]Panjab University, Chandigarh, India
[30]Peking University, Beijing, PR China
[31]Princeton University, Princeton, NJ, USA
[32]University of Science and Technology of China, Hefei, PR China
[33]Seoul National University, Seoul, South Korea
[34]Sungkyunkwan University, Suwon, South Korea
[35]University of Sydney, Sydney, NSW, Australia
[36]Tata Institute of Fundamental Research, Bombay, India
[37]Toho University, Funabashi, Japan
[38]Tohoku Gakuin University, Tagajo, Japan
[39]Tohoku University, Sendai, Japan
[40]Department of Physics, University of Tokyo, Tokyo, Japan
[41]Tokyo Institute of Technology, Tokyo, Japan
[42]Tokyo Metropolitan University, Tokyo, Japan
[43]Tokyo University of Agriculture and Technology, Tokyo, Japan
[44]University of Tsukuba, Tsukuba, Japan
[45]Virginia Polytechnic Institute and State University, Blacksburg, VA, USA
[46]Yonsei University, Seoul, South Korea
[47]University of Tsukuba, Tsukuba

(Dated: February 7, 2008)

Abstract

We have searched for the lepton-flavor-violating decay $\tau \to e\gamma$ using a data sample of 86.7 fb^{-1} collected with the Belle detector at the KEKB asymmetric e^+e^- collider. No evidence for a signal is obtained, and we set an upper limit for the branching fraction $\mathcal{B}(\tau \to e\gamma) < 3.9 \times 10^{-7}$ at the 90% C.L.

PACS numbers: 13.35.Dx, 11.30.Fs, 14.60.Fg

INTRODUCTION

Lepton-flavor-violating (LFV) processes are good probes of physics beyond the Standard Model (SM). For instance, in some supersymmetric models, off-diagonal components of the left-handed slepton mass matrix, $m_{\tilde{L}}$, could radiatively induce LFV such as in $\tau \to \mu(e)\gamma$ and $\mu \to e\gamma$ decays [1, 2]. In general, the branching fraction $\mathcal{B}(\tau \to \mu\gamma)$ is expected to be larger than $\mathcal{B}(\tau \to e\gamma)$, since the mixing between the third and second families is typically assumed to be stronger than that between the third and first families. However, if the first and third families couple more strongly, for instance, due to an inverted hierarchy of slepton masses, then $\mathcal{B}(\tau \to e\gamma)$ could exceed $\mathcal{B}(\tau \to \mu\gamma)$ and might be detectable [3]. Values of $\mathcal{B}(\tau \to e\gamma)$ which can exceed that for $\mathcal{B}(\tau \to \mu\gamma)$ are also predicted in the models with heavy Dirac neutrinos [4, 5]. Thus, a study of both $\tau \to e\gamma$ and $\tau \to \mu\gamma$ decays is essential not only to search for new physics but also to further examine lepton flavor structure.

The decay $\tau \to e\gamma$ has been searched for, along with $\tau \to \mu\gamma$, by MARK II [6], Crystal Ball [7], ARGUS [8], DELPHI [9], and CLEO [10], among which CLEO has set the most sensitive upper limit of $\mathcal{B}(\tau \to e\gamma) < 2.7 \times 10^{-6}$ at 90% C.L.

Recently the Belle collaboration performed a search for the LFV decay $\tau \to \mu\gamma$ [11]. Here we present a new search for the decay $\tau \to e\gamma$ based on data samples of 77.7 fb^{-1} and 9.0 fb^{-1}, collected at the $\Upsilon(4S)$ resonance and in the continuum 60 MeV below the resonance, respectively, equivalent in total to 77.3×10^6 $\tau^+\tau^-$ pairs. The data were collected with the Belle detector at the KEKB asymmetric e^+e^- collider [12]. A description of the detector can be found in Ref. [13].

DATA SELECTION

We search for events containing exactly two oppositely-charged tracks and at least one photon. The events should be consistent with a $\tau^+\tau^-$ event in which one τ (signal side) decays to $e\gamma$ and the other (tag side) decays to a non-electron charged particle (denoted hereafter as $\not{e}$), neutrino(s) and any number of photons.

The selection criteria are determined by studying Monte Carlo (MC) simulations for signal τ-pair decay and background (BG) events, such as generic τ-pair decay ($\tau^+\tau^-$), $q\bar{q}$ continuum, $B\bar{B}$, Bhabha, $\mu^+\mu^-$, and two-photon events [11]. The KORALB/TAUOLA [14] and QQ [15] generators are used for event generation, and the Belle detector response is simulated by a GEANT3 [16] based program. The two-body decay $\tau \to e\gamma$ is initially assumed to have a uniform angular distribution in the τ lepton's rest system.

The selection criteria are similar to those used in the $\tau \to \mu\gamma$ search [11]. Kinematic variables with a CM superscript are calculated in the center-of-mass frame; all other variables are calculated in the laboratory frame. Before electron identification, all the charged tracks are assumed to be pions. Each track is required to have momentum $p^{\rm CM} < 4.5$ GeV/c and momentum transverse to the e^+ beam $p_t > 0.1$ GeV/c, the former requirement being imposed to avoid Bhabha and $\mu^+\mu^-$ contamination. We require that the energy E_γ of each photon exceed 0.1 GeV. In addition, we also require the total energy measured in the CsI(Tl) electromagnetic calorimeter (ECL), $E_{\rm ECL}$, to be less than 9 GeV in order to suppress background from Bhabha events.

The tracks and photons must be detected within the detector's fiducial volume $-0.866 < \cos\theta < 0.956$, but outside the barrel–endcap gaps defined by $0.829 < \cos\theta < 0.880$ and $-0.716 < \cos\theta < -0.602$. Here, θ is the polar angle with respect to the direction opposite

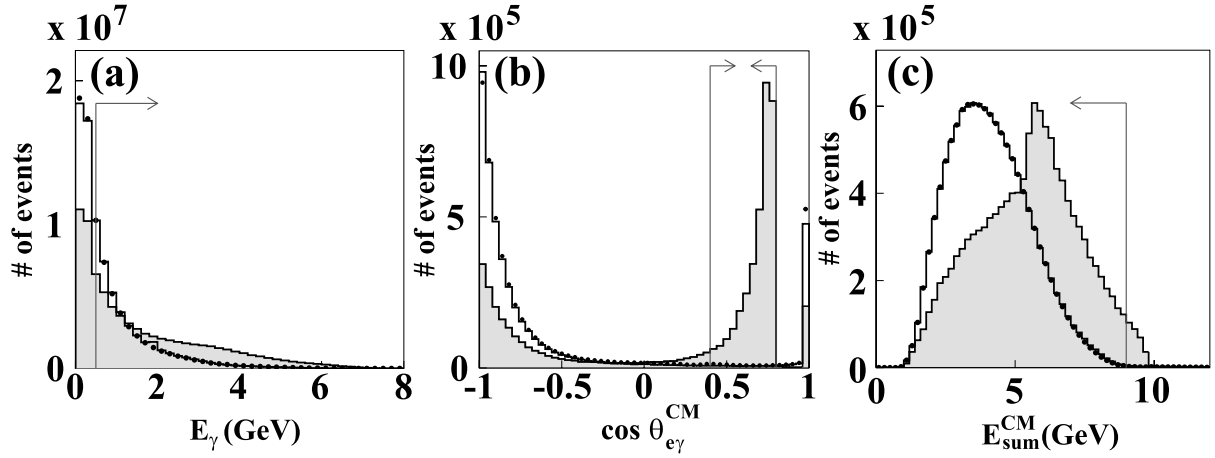

FIG. 1: (a) Energy distribution of the signal candidate photon. (b) $\cos\theta_{e\gamma}^{\rm CM}$ distribution. (c) $E_{\rm sum}^{\rm CM}$ distributions. The open histogram is the sum of backgrounds from generic $\tau^+\tau^-$, $q\bar{q}$ (uds) continuum, Bhabha, $\mu^+\mu^-$ and two-photon processes evaluated from MC simulation. Dots indicate the data distribution, and the shaded histogram is the signal MC distribution. Electron identification requirements were applied for these figures.

to the e^+ beam. Identification of electrons is performed using an electron likelihood ratio, $\mathcal{L}_e$, which is based on the dE/dx information from the central drift chamber (CDC), the ratio of the energy deposited in the ECL to the momentum measured by both the CDC and the silicon vertex detector (SVD), the shower shape in the ECL, the hit information from the aerogel Cherenkov counter, and time-of-flight measurements [17].

The electron track that forms a $\tau \to e\gamma$ candidate (hereafter denoted as $(e\gamma)$) is required to have an e likelihood ratio $\mathcal{L}_{\rm e} > 0.90$ and a momentum $p > 1.0$ GeV/c. This requirement has an efficiency of (93±3)% in the barrel and forward detector and (76±7)% in the backward detector because of the additional material. On the tag side, the $\not{e}$ track is required to have $\mathcal{L}_{\rm e} < 0.1$. The fraction η of electrons with $\mathcal{L}_{\rm e} < 0.1$ is measured to be $(4 \pm 3)\%$ in the barrel and forward detector and $(13 \pm 5)\%$ in the backward detector for $p > 1.0$ GeV/c.

The photon that forms an $(e\gamma)$ candidate is required to have $E_\gamma > 0.5$ GeV in order to reduce spurious combinations of a low-energy γ with an electron, see Fig. 1(a).

A requirement on the cosine of the opening angle between the e and γ of the $(e\gamma)$ candidate, $0.4 < \cos\theta_{e\gamma}^{\rm CM} < 0.8$, is particularly powerful in rejecting the generic $\tau^+\tau^-$ BG events (see Fig. 1(b)). The events in Fig. 1(b) that peak at $\cos\theta_{e\gamma}^{\rm CM} \sim 1$, arise from electrons that radiate a photon when they interact in the SVD or in materials around it. The requirement $E_{\rm sum}^{\rm CM} < 9.0$ GeV is imposed to reject Bhabha and $\mu^+\mu^-$ production, where $E_{\rm sum}^{\rm CM}$ is defined as the sum of the energies of the two charged tracks and the photon composing the $(e\gamma)$, see Fig. 1(c). The opening angle between the two tracks in the laboratory frame is required to be greater than 90°.

We define $\vec{p}_{\rm miss}$ as the residual momentum vector calculated by subtracting the vector sum of all visible momenta (of both tracks and photons) from the vector sum of the beam momenta. Constraints on the momentum and cosine of the polar angle of the missing particle are imposed: $p_{\rm miss} > 0.4$ GeV/c and $-0.866 < \cos\theta_{\rm miss} < 0.956$. To remove $\tau^+\tau^-$ BG events, we apply a requirement on the opening angle between the tagging track and the missing particle of $0.4 < \cos\theta_{{\rm miss}-\not{e}}^{\rm CM} < 0.99$.

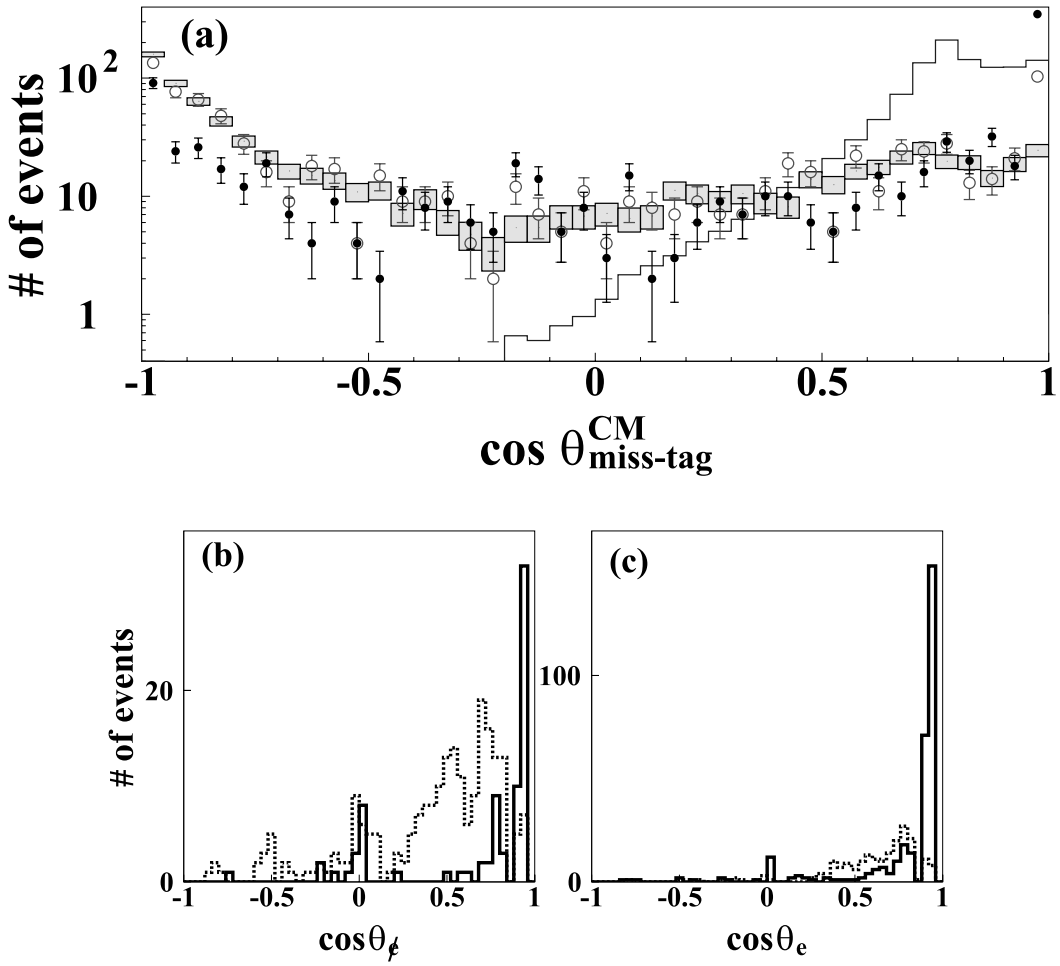

FIG. 2: (a) $\cos\theta^{\rm CM}_{\rm miss-tag}$ distribution. For ℓ-tagged events, the distributions of signal MC (histogram), generic $\tau^+\tau^-$ MC (boxes), and $\ell(e\gamma)$data sample (open circles) are shown. For e-tagged events, the distribution for $e(e\gamma)$ data (closed circles) are also plotted. All requirements except the one for $\cos\theta^{\rm CM}_{\rm miss-tag}$ are applied. (b) $\cos\theta_\ell$ and (c) $\cos\theta_e$ distributions. These are polar angle distributions of the tag side track for $\ell(e\gamma)$ and $e(e\gamma)$ data, respectively, where the solid histogram is for the events with $\cos\theta^{\rm CM}_{\rm miss-tag} > 0.99$ and the dotted histogram is for $0.4 < \cos\theta^{\rm CM}_{\rm miss-tag} < 0.99$ (tagged by e or ℓ).

The upper bound on $\cos\theta^{\rm CM}_{{\rm miss}-\ell}$ is introduced to reject radiative Bhabha events in which one of the electrons forms an $(e\gamma)$ candidate with a radiated photon and the electron on the tag side is misidentified as the ℓ due to the electron identification inefficiency. By analyzing a Bhabha data sample, a large portion of such events is found to have a very small opening angle, $\cos\theta^{\rm CM}_{{\rm miss}-\ell} \simeq 1$, and a polar angle peaking strongly forward, $\cos\theta_\ell > 0.8$. Figure 2(a) shows the $\cos\theta^{\rm CM}_{\rm miss-tag}$ distributions with tag given by ℓ or e for $\ell(e\gamma)$ or $e(e\gamma)$ modes, respectively, in the actual Bhabha data samples, and the signal and generic $\tau^+\tau^-$ MC data. Figures 2 (b) and (c) present the $\cos\theta_{\rm tag}$ distribution for $\ell(e\gamma)$ and $e(e\gamma)$

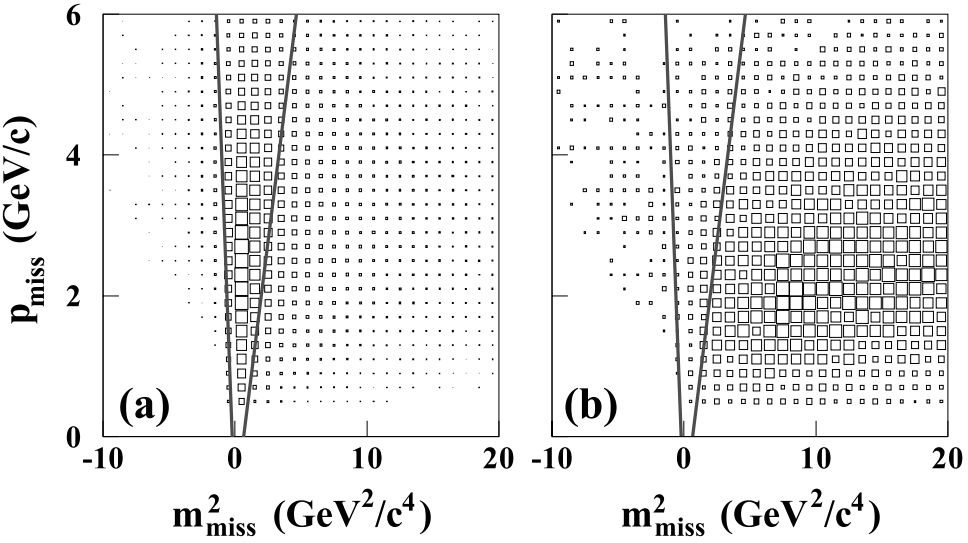

FIG. 3: Event distribution in the $m^2_{\rm miss} - p_{\rm miss}$ plane for (a) signal and (b) generic $\tau^+\tau^-$ MCs. The events within the two lines are accepted in the analysis.

Bhabha data samples, respectively. The requirement, $\cos\theta^{\rm CM}_{\rm miss-tag} < 0.99$, reduces $\not{e}(e\gamma)$ and $e(e\gamma)$ candidates that originate from radiative Bhabhas by 73% and 45%, respectively, while only slightly affecting the signal (97%) and generic $\tau^+\tau^-$ (99%) events.

Finally, a condition is imposed on the relation between $p_{\rm miss}$ and the mass-squared of a missing particle, $m^2_{\rm miss}$. The latter is defined as $E^2_{\rm miss} - p^2_{\rm miss}$, where $E_{\rm miss}$ is 11.5 GeV (the sum of the beam energies) minus the sum of all visible energy and is calculated assuming the electron (pion) mass for the charged track on the signal (tag) side. We require $p_{\rm miss} > -5\ (c^3/{\rm GeV}) \times m^2_{\rm miss} - 1\ ({\rm GeV}/c)$ and $p_{\rm miss} > 1.5\ (c^3/{\rm GeV}) \times m^2_{\rm miss} - 1\ ({\rm GeV}/c)$, where $p_{\rm miss}$ is in GeV/c and $m_{\rm miss}$ is in GeV/c^2 (see Fig. 3). With this cut, 98% of the generic $\tau^+\tau^-$ and 97% of the $e^+e^-\gamma$ backgrounds are removed, while 69% of the signal events remain. In addition, most of the remaining $B\bar{B}$, continuum, and two-photon events are rejected by this requirement.

After these selection requirements, 224 events remain in the data, about 3 times fewer than in the $\tau \to \mu\gamma$ case. Since the inefficiency of electron identification is much smaller than that of the muon, the Bhabha BG is strongly suppressed in spite of its much larger cross-section than that of $e^+e^- \to \mu^+\mu^-\gamma$. The $\tau \to e\gamma$ detection efficiency is evaluated by MC to be 7.29%, about 40% smaller than that of $\tau \to \mu\gamma$, mostly because of the $E_{\rm ECL}$ requirement.

True signal events will have an invariant mass ($M_{\rm inv}$) close to the τ lepton mass and an energy close to the beam energy in the CM frame, i.e., $\Delta E = E^{\rm CM}_{e\gamma} - E^{\rm CM}_{\rm beam} \simeq 0$. When deciding on our selection criteria, we excluded the signal region 1.68 GeV/c^2 $< M_{\rm inv} <$ 1.85 GeV/c^2 so as not to bias our choice of criteria (a "blind" analysis). Only after all requirements were finalized and the number of BG events estimated did we include this region and count the number of signal events.

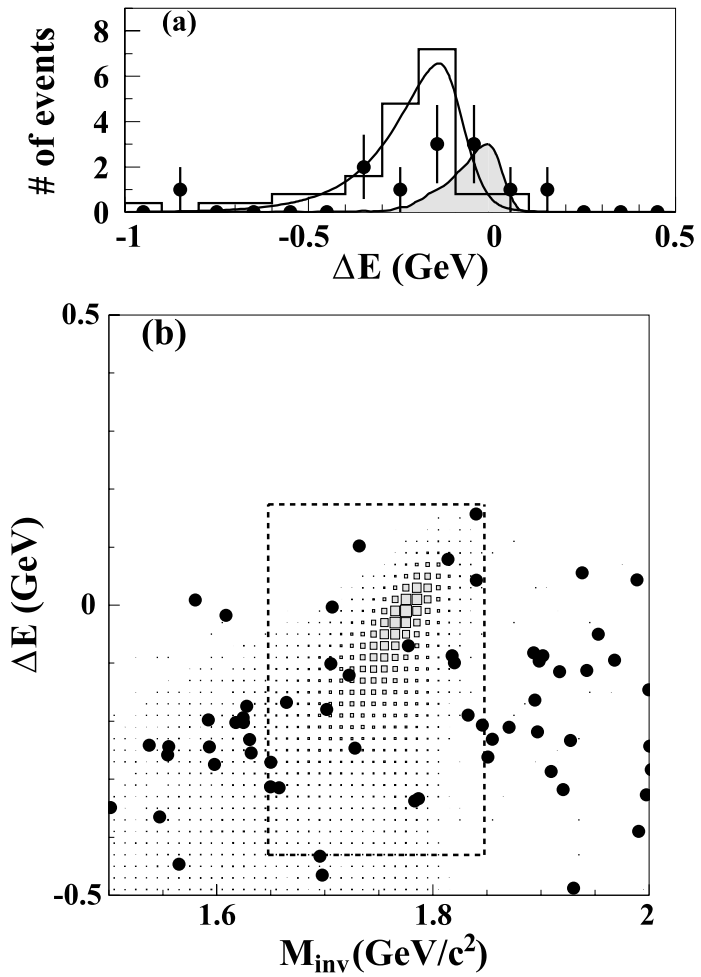

FIG. 4: (a) ΔE distributions for the data (dots) and the expected BG (curve and open histogram) in the blinded region. The distribution for signal MC is the shaded curve. See the text for more detail. (b) $M_{\rm inv}$ *vs.* ΔE distributions for the data (dots) and signal MC (shaded boxes). The $\pm 5\sigma$ region is indicated by the dashed rectangle.

RESULTS

Background Evaluation

To analyze the BG distributions, we define a region, named "grand signal region": -0.5 GeV$< \Delta E < 0.5$ GeV and 1.5 GeV$/c^2 < M_{\rm inv} < 2.0$ GeV$/c^2$, containing 90% of signal MC events passing all previous requirements.

The resolution in ΔE and $M_{\rm inv}$ is evaluated by MC: an asymmetric Gaussian reproduces the dominant part of the signal MC distribution with $\sigma_{\Delta E}^{\rm low/high} = (84.8 \pm 1.2)/(36.0 \pm 0.9)$ MeV and $\sigma_{M_{\rm inv}}^{\rm low/high} = (25.7 \pm 0.3)/(14.3 \pm 0.2)$ MeV$/c^2$, where $\sigma^{\rm low/high}$ means the standard deviation at the lower/higher side of the peak. The peak positions are -6.2 ± 1.0 MeV and 1776.0 ± 0.2 MeV$/c^2$ for ΔE and $M_{\rm inv}$, respectively.

A dominant source of BG is the process $e^+e^- \to \tau^+\tau^-\gamma$, in which the photon is radiated from the initial state: an $(e\gamma)$ candidate is formed by the electron from the $\tau \to e\nu\overline{\nu}$ decay

and the initial state radiation photon, while the tag side τ decays generically via a one-prong mode but not to an electron. From a 174 fb^{-1} sample of MC $\tau^+\tau^-\gamma$ events we find $N^{\tau\tau\gamma} = 60.8 \pm 5.5$ events in the "grand signal region."

The contribution from the process $\not{e}e\gamma$ was described above and is evaluated as $N^{\not{e}e\gamma} = \kappa \times N^{ee\gamma}$, where $\kappa = \eta/(1-\eta)$. From the data $N^{ee\gamma}$ is found to be 68.0 ± 8.2 events and κ is estimated to be 0.06 ± 0.03 from both the Bhabha data and MC samples taking into account the momentum dependence based on the momentum distribution of the signal MC events. Thus, we have $N^{\not{e}e\gamma} = 4.3 \pm 2.0$ events.

From the MC simulation, no other process is expected to contribute to the background. Therefore, the expected BG in the "grand signal region" is 65.1 ± 5.9 events.

The $M_{\rm inv}$ and ΔE shapes of both types of BG events are empirically reproduced by a combination of Landau and Gaussian functions.

For $\tau^+\tau^-\gamma$,

$$N^{\tau\tau\gamma}(M_{\rm inv}, \Delta E) \;=\; \begin{cases} a(M_{\rm inv}) \times \exp\left[-\left(\dfrac{\alpha}{\sqrt{2}\;\upsilon_{\rm h}}\right)^2\right] \\ \qquad\qquad \text{for } \Delta E > \Delta E^{\tau\tau\gamma}_{\rm peak}(M_{\rm inv}), \\ a(M_{\rm inv}) \times \exp\left[\dfrac{1}{2} + \dfrac{1}{2}\left\{\dfrac{\alpha}{\upsilon_{\rm l}} - \exp\left(\dfrac{\alpha}{\upsilon_{\rm l}}\right)\right\}\right] \\ \qquad\qquad \text{for } \Delta E < \Delta E^{\tau\tau\gamma}_{\rm peak}(M_{\rm inv}), \end{cases} \tag{1}$$

and for $e^+e^-\gamma$,

$$N^{ee\gamma}(M_{\rm inv}, \Delta E) \;=\; b(M_{\rm inv}) \times \exp\left[\frac{1}{2} + \frac{1}{2}\left\{\frac{\beta}{\omega_{\rm h/l}} - \exp\left(\frac{\beta}{\omega_{\rm h/l}}\right)\right\}\right] \qquad \text{for } \Delta E \gtrless \Delta E^{\tau\tau\gamma}_{\rm peak}(M_{\rm inv}). \tag{2}$$

Here $\alpha = \Delta E - \Delta E^{\tau\tau\gamma}_{\rm peak}(M_{\rm inv})$ and $\beta = \Delta E - \Delta E^{ee\gamma}_{\rm peak}(M_{\rm inv})$, where $\Delta E_{\rm peak}$ denotes the peak position in terms of $c \times M_{\rm inv} + d$ for individual BG's. The parameters $a, b, c, d, \upsilon_{\rm l/h}$ and $\omega_{\rm l/h}$ are determined from MC for $\tau^+\tau^-\gamma$ and from data for the $e^+e^-\gamma$.

The BG distribution can then be represented by the sum of the two BG components above as

$$N_{\rm BG}(M_{\rm inv}, \Delta E) = N^{\tau\tau\gamma}(M_{\rm inv}, \Delta E) + \kappa \times N^{ee\gamma}(M_{\rm inv}, \Delta E). \tag{3}$$

Figure 4(a) compares the ΔE distribution in the 1.70 GeV/c^2 $< M_{\rm inv} <$ 1.82 GeV/c^2 ($\pm 3\sigma_{M_{\rm inv}}$) region for BG events expected from Eq. (3) (the solid curve) and the events obtained by interpolating the data distribution from both sidebands, 1.53 GeV/c^2 $< M_{\rm inv} <$ 1.68 GeV/c^2 and 1.85 GeV/c^2 $< M_{\rm inv} <$ 2.0 GeV/c^2 (the open histogram). Good agreement between them is observed.

Upper Limit for $\mathcal{B}(\tau \to e\gamma)$

After opening the blinded region, we find the ΔE and $M_{\rm inv}$ *vs.* ΔE distributions that are shown in Figs. 4 (a) and (b), respectively. The number of surviving data events in

the "grand signal region" is 60, in good agreement with the expected BG contribution of 65.1 ± 5.9 events.

In order to extract the number of signal events from the surviving sample, we apply an unbinned extended maximum likelihood fit with the likelihood function defined as

$$\mathcal{L} = \frac{e^{-(s+b)}}{N!} \prod_{i=1}^{N} (sS_i + bB_i), \tag{4}$$

where N is the number of observed events, s and b are free parameters representing the numbers of signal and BG events to be extracted, respectively, and $S_i \equiv S(M_{\rm inv}^{(i)}, \Delta E^{(i)})$ and $B_i \equiv B(M_{\rm inv}^{(i)}, \Delta E^{(i)})$ are the signal and BG probability density functions for the i-th event. The function $B(M_{\rm inv}, \Delta E)$ is taken from Eq. (3) while $S(M_{\rm inv}, \Delta E)$ is obtained by generating 10^6 signal MC events.

We apply this fit for s and b to a $\pm 5\sigma$ region in $M_{\rm inv}$ and ΔE: 1.65 GeV/c^2 $< M_{\rm inv} <$1.85 GeV/c^2 and -0.43 GeV $< \Delta E <$0.17 GeV. There are a total of 20 events in this region while 25.7 ± 0.3 events are expected from Eq. (3), and, when s is constrained to be non-negative, the fit finds $s = 0$ and $b = 20.0$.

To calculate the upper limit, Monte Carlo samples are generated by fixing the expected number of BG events ($\tilde{b}$) to the value $b = 20$. For every assumed expected number of signal events ($\tilde{s}$), 10,000 samples are generated, for each of which the numbers of signal and BG events are determined by Poisson statistics with means $\tilde{s}$ and $\tilde{b}$, respectively. We then assign $M_{\rm inv}$ and ΔE values to these events according to their density distributions. An unbinned maximum likelihood fit is performed for every sample to extract the number of signal events ($s^{\rm MC}$). The confidence level for an assumed $\tilde{s}$ is defined as the fraction of the samples whose $s^{\rm MC}$ exceeds s. This procedure is repeated until we find the value of $\tilde{s}$ ($\tilde{s}_{90}$) that gives a 90% chance of $s^{\rm MC}$ being larger than s.

The resulting upper limit at 90% C.L. is $\tilde{s}_{90} = 3.75$ events. An upper limit on the branching fraction is obtained via the formula:

$$\mathcal{B}(\tau \to e\gamma) < \frac{\tilde{s}_{90}}{2\epsilon N_{\tau\tau}}, \tag{5}$$

where $N_{\tau\tau}$ is the total number of τ-pairs produced, and ϵ is the detection efficiency in the $\pm 5\sigma$ region. Inserting the values $N_{\tau\tau} = 77.3 \times 10^6$ and $\epsilon = 6.37\%$ gives $\mathcal{B}(\tau \to e\gamma) < 3.8 \times 10^{-7}$.

Systematic Uncertainties

Systematic uncertainties on $\tilde{s}_{90}$ are evaluated by varying all parameters of the BG probability density function. The fractions of $N^{\tau\tau\gamma}(M_{\rm inv}, \Delta E)$ and $N^{ee\gamma}(M_{\rm inv}, \Delta E)$ in Eq. (3) are varied by $\pm 20\%$ and $\pm 100\%$, respectively, about double their estimated uncertainties. As a result, $\tilde{s}_{90}$ varies by $+0.01/-0.00$ and $+0.01/-0.02$ events, respectively. The functional form of the BG spectra is scaled by 1.15 or 0.90 times for $N^{\tau\tau\gamma}(M_{\rm inv}, \Delta E)$ and by 1.3 or 0.6 times for $N^{ee\gamma}(M_{\rm inv}, \Delta E)$, and their centers are shifted by $+0.01/-0.015$ GeV for $N^{\tau\tau\gamma}(M_{\rm inv}, \Delta E)$ and by ± 0.1 GeV for $N^{ee\gamma}(M_{\rm inv}, \Delta E)$, all changes corresponding to the estimated errors of the involved parameters. The shift of the central value for the $N^{\tau\tau\gamma}(M_{\rm inv}, \Delta E)$ spectrum yields the largest effect of $+0.07/-0.13$ events, and the overall systematic uncertainty increasing the upper limit of $\tilde{s}_{90}$ is evaluated as $+0.07$ events. The stability of the result for the

fit region is examined by extending the $M_{\rm inv}$-ΔE region from $\pm 4\sigma$ to $\pm 8\sigma$: no appreciable difference in the upper limit is found.

The systematic uncertainties on the detection sensitivity, $2\epsilon N_{\tau\tau}$, arise from the photon reconstruction efficiency (3.0%), the selection criteria (2.5%), the trigger efficiency (2.0%), the track reconstruction efficiency (2.0%), the luminosity (1.4%), and the MC statistics (0.3%). The total uncertainty is obtained by adding all of these components in quadrature; the result is 5.0%. The contribution of the largest component, the photon reconstruction efficiency, is evaluated from the $e^+e^-\gamma$ data sample. The uncertainty of the selection criteria is estimated by varying the required polar angle region of the signal candidate photon. The trigger efficiency is estimated from the difference between a $\tau^+\tau^-$ data sample and a generic $\tau^+\tau^-$ MC sample.

These uncertainties are included in the upper limit on $\mathcal{B}(\tau \to e\gamma)$ following [18]. The systematic uncertainty in the efficiency is assumed to have a Gaussian distribution.

While the angular distribution of the $\tau \to e\gamma$ decay is assumed to be uniform in this analysis, it is sensitive to the LFV interaction structure [19], and spin correlations between the τ leptons on the signal and tag sides must be considered. To evaluate the maximum possible variation, $V - A$ and $V + A$ interactions are assumed; no statistically significant difference in the $M_{\rm inv}$-ΔE distribution or in the efficiency is found compared to the case of the uniform distribution. Therefore, systematic uncertainties due to these effects are neglected in the upper limit evaluation.

The incorporation of all systematic uncertainties increases the upper limit by 2.1%. As a result, the upper limit on the branching fraction is

$$\mathcal{B}(\tau \to e\gamma) < 3.9 \times 10^{-7} \qquad \text{at } 90\% \text{ C.L.} \tag{6}$$

SUMMARY

This result improves the sensitivity to the branching fraction by approximately one order of magnitude compared to previous measurements. Despite a smaller detection efficiency compared to $\tau \to \mu\gamma$, the superior BG rejection for electrons allows us to reach a sensitivity for $\tau \to e\gamma$ that is comparable to $\tau \to \mu\gamma$.

Acknowledgements

We thank the KEKB group for the excellent operation of the accelerator, the KEK cryogenics group for the efficient operation of the solenoid, and the KEK computer group and the National Institute of Informatics for valuable computing and Super-SINET network support. We are grateful to A.Ilakovac for fruitful discussions. We acknowledge support from the Ministry of Education, Culture, Sports, Science, and Technology of Japan and the Japan Society for the Promotion of Science; the Australian Research Council and the Australian Department of Education, Science and Training; the National Science Foundation of China under contract No. 10175071; the Department of Science and Technology of India; the BK21 program of the Ministry of Education of Korea and the CHEP SRC program of the Korea Science and Engineering Foundation; the Polish State Committee for Scientific Research under contract No. 2P03B 01324; the Ministry of Science and Technology of the

Russian Federation; the Ministry of Education, Science and Sport of the Republic of Slovenia; the Swiss National Science Foundation; the National Science Council and the Ministry of Education of Taiwan; and the U.S. Department of Energy.

---

* on leave from Nova Gorica Polytechnic, Nova Gorica

[1] R. Barbieri and L. J. Hall, Phys. Lett. B 338 (1994) 212.
[2] J. Hisano et al., Phys. Lett. B 357 (1995) 579.
[3] J. Ellis et al., Phys. Rev. D 66 (2002) 115013.
[4] M.C. Gonzalez-Garcia and J.W.F. Valle, Mod. Phys. Lett. A 7 (1992) 477.
[5] A. Ilakovac, Phys. Rev. D 62 (2000) 036010.
[6] K.G. Hayes et al., MARK II Collaboration, Phys. Rev. D 25 (1982) 2869.
[7] S. Keh et al., Crystal Ball Collaboration, Phys. Lett. B 212 (1988) 123.
[8] H. Albrecht et al., ARGUS Collaboration, Z. Phys. C 55 (1992) 179.
[9] P. Abreu et al., DELPHI Collaboration, Phys. Lett. B 359 (1995) 411.
[10] K.W. Edwards et al., CLEO Collaboration, Phys. Rev. D 55 (1997) R3919.
[11] K. Abe et al., Belle Collaboration, Phys. Rev. Lett. 92 (2004) 171802.
[12] S. Kurokawa and E. Kikutani, Nucl. Instr. Meth. A 499 (2003) 1, and other papers included in this Volume.
[13] A. Abashian et al., Belle Collaboration, Nucl. Instr. Meth. A 479 (2002) 117.
[14] S. Jadach and Z. Wąs, Comp. Phys. Commun. 85 (1995) 453.
[15] http://www.lns.cornell.edu/public/CLEO/soft/QQ.
[16] R. Brun, et al., GEANT 3.21, CERN Report No. DD/EE/84-1 (1987).
[17] K. Hanagaki et al., Nucl. Instr. Meth. A 485 (2002) 490.
[18] S. Ahmed et al., CLEO Collaboration, Phys. Rev. D 61 (2000) 071101(R).
[19] R. Kitano and Y. Okada, Phys. Rev. D 63 (2001) 113003.